infinite array scans to $\theta = 45^0$ in the E-, H-, and D-planes across a $13.3:1$ bandwidth ($VSWR \leq 3$). The design was validated through extensive measurements of a fabricated 8×8 prototype array.

REFERENCES

[1] G. C. Tavik, C. L. Hilterbrick, J. B. Evins, J. J. Alter, J. G. Crnkovich, J. W. d. Graff, W. Habicht, G. P. Hrin, S. A. Lessin, D. C. Wu, and S. M. Hagewood, "The advanced multifunction RF concept," *IEEE Trans. Microwave Theory Tech.*, vol. 53, no. 3, pp. 1009–1020, 2005.

[2] P. S. Hall, P. Gardner, and A. Faraone, "Antenna requirements for software defined and cognitive radios," *Proc. IEEE*, vol. 100, pp. 2262–2270, 2012.

[3] K. E. Browne, R. J. Burkholder, and J. L. Volakis, "Through-wall opportunistic sensing system utilizing a low-cost flat-panel array," *IEEE Trans. Antennas Propag.*, vol. 59, no. 3, pp. 859–868, 2011.

[4] W. F. Croswell, T. Durham, M. Jones, D. Schaubert, P. Friederich, and J. G. Maloney, "Wideband arrays," in *Modern Antenna Handbook*, C. A. Balanis, Ed. New York, NY, USA: Wiley-Interscience, 2008, pp. 581–627.

[5] J. P. Doane, K. Sertel, and J. L. Volakis, "A 6.3:1 bandwidth scanning tightly coupled dipole array with co-designed compact balun," presented at the IEEE Int. Symp. on Antennas and Propagation (APSURSI), 2012.

[6] S. S. Holland and M. N. Vouvakis, "The planar ultrawideband modular antenna (PUMA) array," *IEEE Trans. Antennas Propag.*, vol. 60, no. 1, pp. 130–140, 2012.

[7] M. Jones and J. Rawnick, "A new approach to broadband array design using tightly coupled elements," in *Proc. IEEE MILCOM*, Oct. 29–31, 2007, pp. 1–7.

[8] J. J. Lee, "Ultra wideband arrays," in *Antenna Engineering Handbook*, J. L. Volakis, Ed., 4th ed. New York, NY, USA: McGraw Hill, 2007.

[9] B. A. Munk, *Finite Antenna Arrays and FSS*. Piscataway/Hoboken, NJ, USA: IEEE Press/Wiley-Interscience, 2003 , ch. 6, pp. 181–213.

[10] W. F. Moulder, K. Sertel, and J. L. Volakis, "Superstrate-enhanced ultrawideband tightly coupled array with resistive FSS," *IEEE Trans. Antennas Propag.*, vol. 60, no. 9, pp. 4166–4172, 2012.

[11] D. Cavallo, A. Neto, and G. Gerini, "PCB slot based transformers to avoid common-mode resonances in connected arrays of dipoles," *IEEE Trans. Antennas Propag.*, vol. 58, no. 8, pp. 2767–2771, 2010.

[12] H. A. Wheeler, "The radiation resistance of an antenna in an infinite array or waveguide," *Proc. IRE*, vol. 36, no. 5, pp. 478–487, 1948.

[13] D. G. Bodnar, "Materials and design data," in *Antenna Engineering Handbook*, J. L. Volakis, Ed., 4th ed. New York, NY, USA: McGraw Hill, 2007.

[14] W. K. Roberts, "A new wide-band balun," *Proc. IRE*, vol. 45, no. 12, pp. 1628–1631, 1957.

[15] A. C. Chen, M. J. Chen, and A. V. Pham, "Design and fabrication of ultra-wideband baluns embedded in multilayer liquid crystal polymer flex," *IEEE Trans. Adv. Packag.*, vol. 30, no. 3, pp. 533–540, 2007.

[16] J. H. Cloete, "Exact design of the Marchand balun," in *Proc. 9th Eur. Microwave Conf.*, 1979, pp. 480–484.

[17] N. Marchand, "Transmission-line conversion transformers," *Electronics*, vol. 17, no. 12, pp. 142–145, 1944.

[18] D. M. Pozar, *Microwave Engineering*, 3 ed. Hoboken, NJ, USA: Wiley, 2005, ch. 4, pp. 161–221.

[19] T. S. Chen, "Determination of the capacitance, inductance, and characteristic impedance of rectangular lines," *IRE Trans. Microwave Theory Tech.*, vol. 8, no. 5, pp. 510–519, 1960.

[20] D. M. Pozar, *Microwave Engineering*. Hoboken, NJ, USA: Wiley, 2005, ch. 5, pp. 258–261.

[21] R. W. Klopfenstein, "A transmission line taper of improved design," *Proc. IRE*, pp. 31–36, 1956.

[22] A. Ludwig, "The definition of cross polarization," *IEEE Trans. Antennas Propag.*, vol. 21, no. 1, pp. 116–119, 1973.

[23] C. A. Balanis, *Advanced Engineering Electromagnetics*. Hoboken, NJ, USA: Wiley, 1989, ch. 2, p. 79.

[24] *Antenna Theory: Analysis and Design*, 3 ed. Hoboken, NJ, USA: Wiley, 2005, ch. 17 , pp. 1033–1034.

[25] H. Holter and H. Steyskal, "On the size requirement for finite phased-array models," *IEEE Trans. Antennas Propag.*, vol. 50, no. 6, pp. 836–840, 2002.

[26] W. F. Moulder, K. Sertel, and J. L. Volakis, "Finite size effects on the performance of ultrawideband tightly coupled arrays," presented at the 29th Int. Review of Applied Computational Electromagnetics Society (ACES) Symp., Columbus, OH, USA, 2012.

[27] D. F. Kelley and W. L. Stutzman, "Array antenna pattern modeling methods that include mutual coupling effects," *IEEE Trans. Antennas Propag.*, vol. 41, no. 12, pp. 1625–1632, 1993.

Excitation Control Method for a Low Sidelobe SIW Series Slot Array Antenna With 45° Linear Polarization

Dong-yeon Kim and Sangwook Nam

***Abstract*—A sidelobe suppression method for a series slot array antenna which radiates 45°-inclined linear polarization is proposed. Axial displacements are employed to create arbitrary excitation coefficients for individual centered-inclined radiating slots along the center line of a broad wall. To verify the proposed design method, we design two types of center-fed linear slot array antennas with a Dolph-Chebyshev distribution for –20 dB and –26 dB sidelobe levels (SLLs) in the Ka band. Furthermore, a cross-validation process involving an equivalent circuit model analysis and electromagnetic full-wave simulation using CST MWS is utilized. The entire structure of the proposed series slot array antenna is fabricated on printed circuit boards (PCBs), including drilling and chemical etching, to secure advantages of miniaturization and cost reduction. The measured realized gains are 15.17 and 15.95 dBi and SLLs are –18.7 and –22.5 dB respectively for two types of fabricated antennas. It demonstrates the validity of the proposed sidelobe suppression method.**

***Index Terms*—45 degree linear polarization, millimeter wave antenna, sidelobe suppression, slot array antenna, substrate integrated waveguide.**

I. INTRODUCTION

Waveguide-fed slot array antennas are quite suitable for millimeter-wave radiating systems that require not only high gain, efficiency, and a robust structure but also low cross-polarization and sidelobe levels (SLLs). Despite the above advantages, three-dimensional metallic waveguide slot array antennas are associated with massive volumes, complex manufacturing, and a high cost. Recently, alternative solutions for efficient millimeter-wave antenna manufacturing processes have been studied, such as a "laminated waveguide" or a "substrate integrated waveguide" (SIW) with low conduction and radiation losses[1], [2], [3]. Owing to their simple manufacturing process, involving only drilling and chemical etching on a general printed circuit board (PCBs), low-cost, simply fabricated, and lightweight features are possible. Furthermore, SIW transmission lines are especially compatible with complex feeding networks compared to conventional microstrip transmission lines for millimeter-wave antenna systems due to their low radiation leakage, which typically deteriorates their inherent radiation characteristics. As a result, many

Manuscript received January 21, 2013; revised April 18, 2013; accepted July 30, 2013. Date of publication August 07, 2013; date of current version October 28, 2013. This work was supported by the MSIP (Ministry of Science, ICT & Future Planning), Korea in the ICT R&D Program 2013.

The authors are with the Institute of New Media Communication (INMC), School of Electrical Engineering and Computer Science, Seoul National University, Seoul 151-742, Korea (e-mail: dongyeonkim0818@gmail.com; snam@snu.ac.kr).

Color versions of one or more of the figures in this communication are available online at http://ieeexplore.ieee.org.

Digital Object Identifier 10.1109/TAP.2013.2277711

recent studies of SIW slot array antenna designs have been conducted [4]–[9].

Slot array antennas with highly accurate 45°–inclined linear polarization (LP) are promising candidates for collision avoidance systems as well as dual-polarized radar systems. In these antennas, lower SLLs and higher cross-polarization discrimination (XPD) should be imposed for compatibility against the surrounding electromagnetic (EM) environment effect, such as ghost effects. The SLLs of conventional resonant (i.e., resonantly spaced with a half guided-wavelength) shunt and series slot array antennas can be suppressed by the excitation control using the offsets and tilt angles of every slot because the self-conductance and -resistance of individual shunt and series resonant slots are the function of offsets and tilt angles, respectively [11], [12].

In contrast with the conventional SLL suppression method for the radiating elements having resonant length, we propose the SLL suppression method based on a uniform series slot array antenna suggested in [8] by the authors using axial displacements for inductively and capacitively loaded slots along the center line of a broad wall. The axial displacements control the mode currents on reactively loaded radiating slots, allowing arbitrary excitation coefficients to be determined. As a conventional structure for a uniform 45°–inclined LP, a previously suggested resonantly excited series slot array antenna which has a constant slot spacing distance with a half guided-wavelength is considered in the application of the axial displacement parameters. Also, the validity of the proposed method is evaluated from the calculation results using an equivalent circuit analysis and a commercially available full-wave EM simulation (CST MWS) [13]. Two types of low SLL linear slot array antennas with Dolph-Chebyshev polynomials for –20 dB and –26 dB SLLs are designed and evaluated in terms of the measured electrical performances of the reflection coefficients, realized gains, XPDs, and SLLs.

II. Antenna Structure For Sidelobe Suppression

A conventional uniform linear series slot array antenna is shown in Fig. 1(a). In this antenna, 16 centered-inclined radiating slots (i.e., 8 alternating reactance slot pairs) are separated with the half guided-wavelength of a radiating SIW as a resonantly excited feature. As a result, these radiating units ensure stable radiation characteristics without any grating lobes in the longitudinal direction (*zx* plane). In addition, the symmetric radiation patterns can be guaranteed due to their center-fed structure from a series-to-series coupling slot that is located between a radiating and a feeding SIW, as shown in Fig. 1[8, Fig. 5].

The excitation coefficient design starts from a conventional uniform linear slot array antenna [Fig. 1(a)] using the axial displacements along the longitudinal axis (x–axis) of a radiating SIW, as shown in Fig. 1(b). Eight resonantly spaced radiating slots on the left side of a radiating SIW are numbered from the shorted end to the center of a series-to-series coupling slot location. Furthermore, the axial displacements are set for the inductive (even n) and capacitive (odd n) slots with inward and outward directions of (x_2, x_4, x_6, x_8) and (x_1, x_3, x_5, x_7), respectively, from the resonantly excited positions. All of these displacement values are symmetric with respect to the center of the antenna.

In our research, two types of PCBs with the same dielectric constant of 3.5 are used for a radiating and a feeding SIW with different thicknesses of 1.52 mm and 0.75 mm, respectively. They are precisely aligned using adhesive film with a dielectric constant of 2.35 and a thickness of 38 μm. In order to construct the SIW transmission line as a perfectly electric side wall, metallic via arrays are periodically arranged with a diameter of 0.4 mm and a spacing of 0.7 mm for both the radiating and feeding SIW. These blind vias of a multi-layered antenna structure are constructed using sequential lamination method to develop SIW transmission lines. Also, the width of these SIWs is set to 3.44 mm, making the guided-wavelength (λ_g) therefore 6.8 mm.

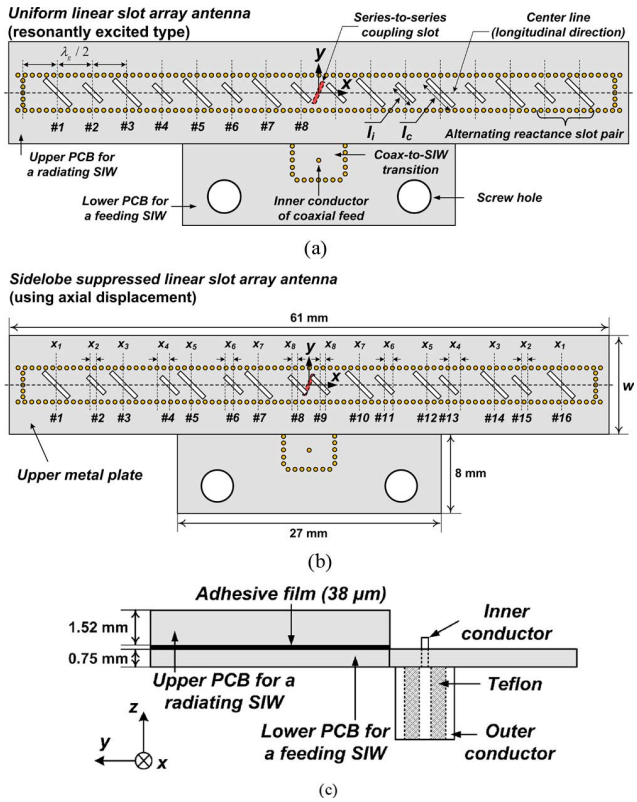

Fig. 1. SIW linear slot array antenna structures (a) for a uniform field distribution [8] and (b) for arbitrary excitation coefficients using axial displacements (from x_1 to x_8). In this case, the axial displacements are employed just for inductive radiating slots (x_2, x_4, x_6, x_8) not capacitive radiating slots (x_1, x_3, x_5, x_7). (c) Side view.

As a result, the fundamental TE_{10} mode at an operating frequency of 35 GHz is able to propagate along the SIW transmission line above a cut-off frequency of 25.06 GHz without any higher-order modes.

III. Excitation Control Method for a low Sidelobe

The centered-inclined radiating slot is modeled as series-connected impedance, which can be extracted using the s-parameters from a two-port network with respect to variation in the length (l_n) and tilt angle (θ_n) [10]. Before the axial displacements are set for the radiating slots, the slot length of an alternating reactance slot pair as a radiating unit should be determined for a uniform field distribution and for input impedance matching. In order to determine the length of an alternating reactance slot pair more precisely, an equation for the slot voltage is required. This is shown below [12]:

$$V_n^s = \frac{z_n \cdot I_n}{K_1 \cdot f(\theta_n, l_n)}. \tag{1}$$

Here, z_n is the normalized self-impedance of the radiating slot, I_n is the mode current, and K_1 and f can be obtained from (5) to (7) as given in earlier work [12]. In our research, the tilt angle of the centered-inclined radiating slot is fixed at $\pi/4$ for 45°–inclined linear polarization. Moreover, the length of the inductive (l_i) and capacitive (l_c) radiating slots as an alternating reactance slot pair should be obtained from the condition of $|V_i^s| = |V_c^s|$ for a uniform distribution. The phase difference between these two resonantly spaced radiating slots is also determined by their own self-impedances, because the mode currents that flow through these series slots are common except for the alternation of their signs [8], [9].

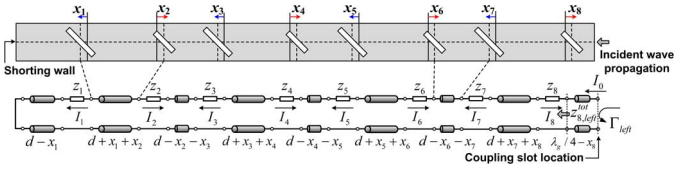

Fig. 2. Equivalent rectangular waveguide slot array model with axial displacements on each radiating slots and its transmission line circuit model.

After the uniform linear slot array antenna is designed, the excitation coefficients between adjacent radiating slots can be determined by the mode current ratio using axial displacement.

$$\frac{|V_n^s|}{|V_{n+1}^s|} = \frac{|I_n|}{|I_{n+1}|} \cdot \left[\frac{|z_n|}{|z_{n+1}|} \cdot \frac{f\left(\frac{\pi}{4}, l_{n+1}\right)}{f\left(\frac{\pi}{4}, l_n\right)} \right]. \tag{2}$$

Because the self-impedances ($z_{\rm n}$ and $z_{\rm n+1}$) and length ($l_{\rm n}$ and $l_{\rm n+1}$) of the slots are already set for a uniform field distribution from (1), the term in the brackets in (2) is unity. Therefore, the mode current expression is required as a function of the axial displacement to formulate an arbitrary field distribution for low sidelobes. Theoretically, the resonant radiating slots are excited by the maximum currents on the broad wall of the conventional series slot array antenna and the excitation coefficients are determined by the tilt angle [12]. In contrast with the conventional series slot array antenna, the proposed series antenna is composed of the non-resonant radiating slots for 45°–inclined LP. When axial displacements are employed on the non-resonant radiating slots, more power can be radiated than they are excited at the original position since the maximally excited current positions inside the radiating waveguide are changed by their series connected inductive or capacitive reactance.

Fig. 2 shows the equivalent radiating RWG for the left side of the proposed center-fed linear slot array antenna and its equivalent circuit below. There are four alternating reactance slot pairs with axial displacements ($x_{\rm n}$) along the center line of a broad wall. Once the axial displacements are applied to each radiating slots, the length of the transmission lines between adjacent series-connected impedances are changed, as shown in Fig. 2. When we know the inductive and capacitive self-impedances of an alternating reactance slot pair, the total input impedance looking from the 8th radiating slot toward the shorted end can be calculated using an impedance recursive formula as a function of the axial displacement:

$$\begin{aligned} z_{1,left}^{tot} &= z_1 + j\tan\left[\beta_{10}\left(d - x_1\right)\right] \\ z_{n,left}^{tot} &= z_n + \frac{z_{n-1,left}^{tot} + j\tan\left[\beta_{10}\left(d + (-1)^n \cdot u_{n-1}\right)\right]}{1 + jz_{n-1,left}^{tot} \cdot \tan\left[\beta_{10}\left(d + (-1)^n \cdot u_{n-1}\right)\right]} \\ &\quad for\ n = 2, 3, \ldots. \end{aligned} \tag{3}$$

In this equation, β_{10} is the propagation constant of the fundamental TE $_{10}$ mode for a given radiating SIW and $d = \lambda_{\rm g}/2$ is set for 3.4 mm at an operating frequency of 35 GHz. Also, the index $u_n = x_{\rm n-1} + x_{\rm n}$ represents the length variation of each transmission line between neighboring radiating slots due to the axial displacement.

The mode currents of each series slot module can be defined by the following recursive formula, see (4) at the bottom of the following page, where I_0 is the input current coupled from a series-to-series coupling slot. The impedance and current recursive formulas can be also employed for the right side of a radiating SIW due to their symmetric feature with respect to the center of an antenna, the location of the series-to-series coupling slot. Finally, substitution of (3) and (4) into (1) yields the magnitudes and phases of the slot voltages applied by the axial displacements.

Meanwhile, the magnitude and phase difference effects of radiating electric fields with respect to the direction of the axial displacements for inductive [x_8 (for slot #8, 9)] and capacitive slots [x_7 (for slot #7, 10)] are investigated using an EM full-wave simulator, CST MWS and equivalent circuit analysis. At this point, the remaining radiating slots are resonantly excited with one-half guided-wavelength spacing. In order to identify the near-field distribution generated by the radiating slots, we set a tracking line 1 mm above a broad wall along the center line of a radiating SIW (x–axis).

As a first example, the single-axial displacement of x_8 for only the two inductive radiating slots of #8 and #9 are adjusted with random values of ± 0.7 mm. In this case, the positive sign indicates that the axial displacement of x_8 moves toward a coupling slot. When a positive x_8 is employed, the magnitudes of the inductive slot voltages are increased until they are nearly double the values of other values, as shown in Fig. 3(a). In addition, the phases of their electric fields approach the phases of the capacitive radiating slots. It is important to note that the centered axial displacements scarcely affect the field distribution of the remaining radiating slots. On the other hand, when two inductive slots move toward both ends of the radiating SIW, the magnitudes of their electric fields are inversely proportional to the remaining slots and the phase differences with the neighboring capacitive slots (slot #7 and #10) are increased considerably. Therefore, the axial displacement for the inductive slots should be employed toward the center of a linear slot array antenna in order to realize a tapered distribution and a decreased phase difference at the same time.

As the next example, axial displacement of x_7 is applied for only two capacitive radiating slots, slots #7 and #10, simultaneously. The positive sign for x_7 means that the capacitive slots are moving toward both ends of a radiating SIW. Regarding the magnitudes of the radiated electric fields, there is an insufficient distribution to suppress the sidelobes, especially in the case of negative axial displacement. In addition, for the phase difference, it is obvious that the phase difference as regards the neighboring inductive radiating slots (slots #8 and #9) increases to more than 40° regardless of the direction of the axial displacement. Consequently, it is suitable and highly advantageous to apply the axial displacement only for the inductive radiating slots associated with the magnitude and phase distribution. From the viewpoint of phase, the

$$\begin{aligned} I_8 &= \frac{I_0}{\cos\left[\beta_{10}\left(d - x_8\right)\right] + jz_{8,left}^{tot} \cdot \sin\left[\beta_{10}\left(d - x_8\right)\right]} \\ I_n &= \frac{I_{n+1}}{\cos\left[\beta_{10}\left(d - (-1)^n \cdot u_{n+1}\right)\right] + jz_{n,left}^{tot} \cdot \sin\left[\beta_{10}\left(d - (-1)^n \cdot u_{n+1}\right)\right]} \\ &\quad for\ n = 7, 6, \ldots 1 \end{aligned} \tag{4}$$

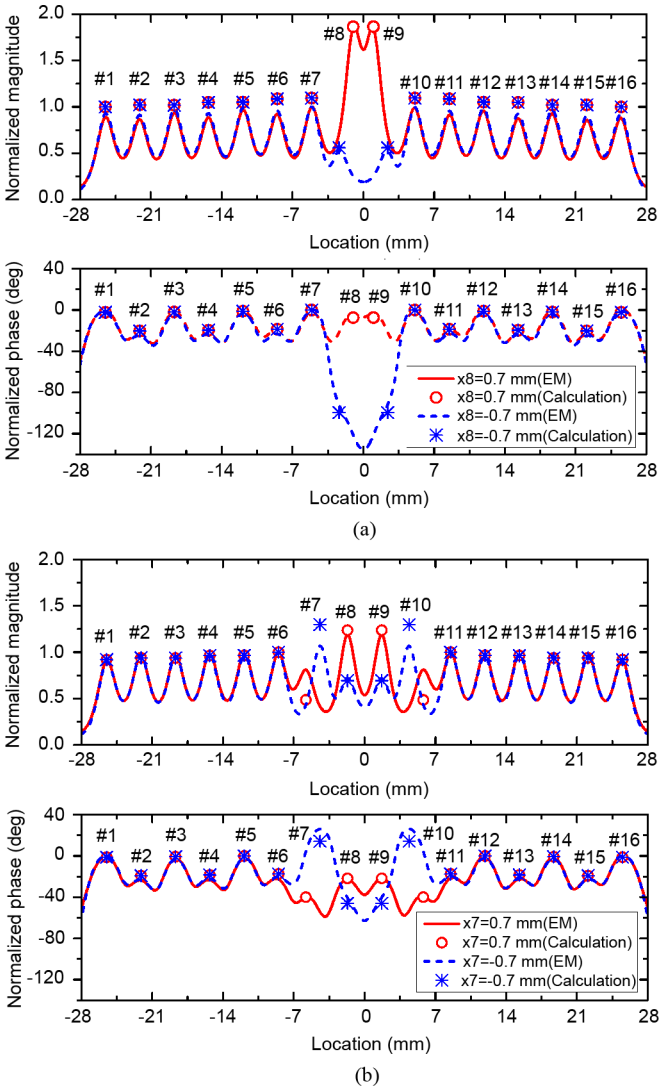

Fig. 3. The magnitude and phase variation of radiating electric fields with respect to the direction of axial displacements for (a) inductive (slots #8 and #9) and (b) capacitive (slots #7 and #10) radiating slots, respectively. For the verification, the calculated results from recursive formulas are depicted.

properly increased distance between reactively loaded radiating slots compensates their phase difference compared with the spacing of one-half guided-wavelength.

IV. Design Procedure For Excitation Control

We realize a Dolph-Chebyshev distribution for –20 dB and –26 dB sidelobes using the proposed axial displacement scheme. As mentioned in the previous section, the tapered excitation coefficients can be easily controlled by the axial displacement for inductive radiating slots. In order to fit into a smoothly decreasing curve such as a cosine function, the axial displacements are successively adopted from the center of a linear slot array antenna, as shown in Fig. 4.

When the axial displacement of $x_8 = 0.2$ mm is employed for radiating slots #8 and #9, the magnitudes and phase differences are tapered and reduced, respectively. On the other hand, the others are conserved in the form of a uniform field distribution, as shown in Fig. 4(a). The next step is to set the axial displacements of x_6 and x_4 sequentially at 0.25 mm and 0.8 mm, respectively. As depicted in Fig. 4(b) and (c), the tapered excitation coefficients can be controlled independently from slots #4 to #13, except for the remaining respective three radiating slots located in both shorted walls.

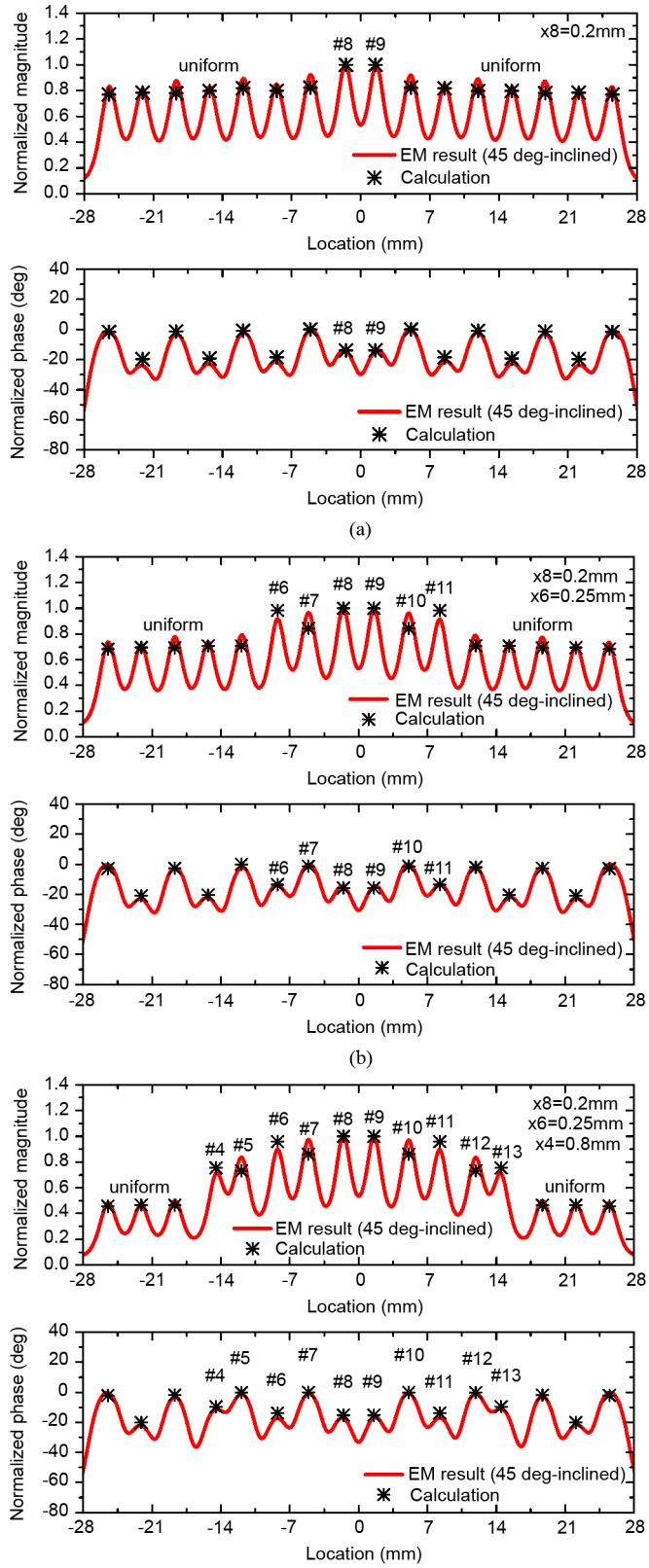

Fig. 4. The slot voltage characteristics according to the progressive axial displacement variations. The calculated results from the equivalent circuit are shown with EM results.

The inversely proportional excitation coefficient is required for –20 dB SLL for the precise design of the excitation coefficients,

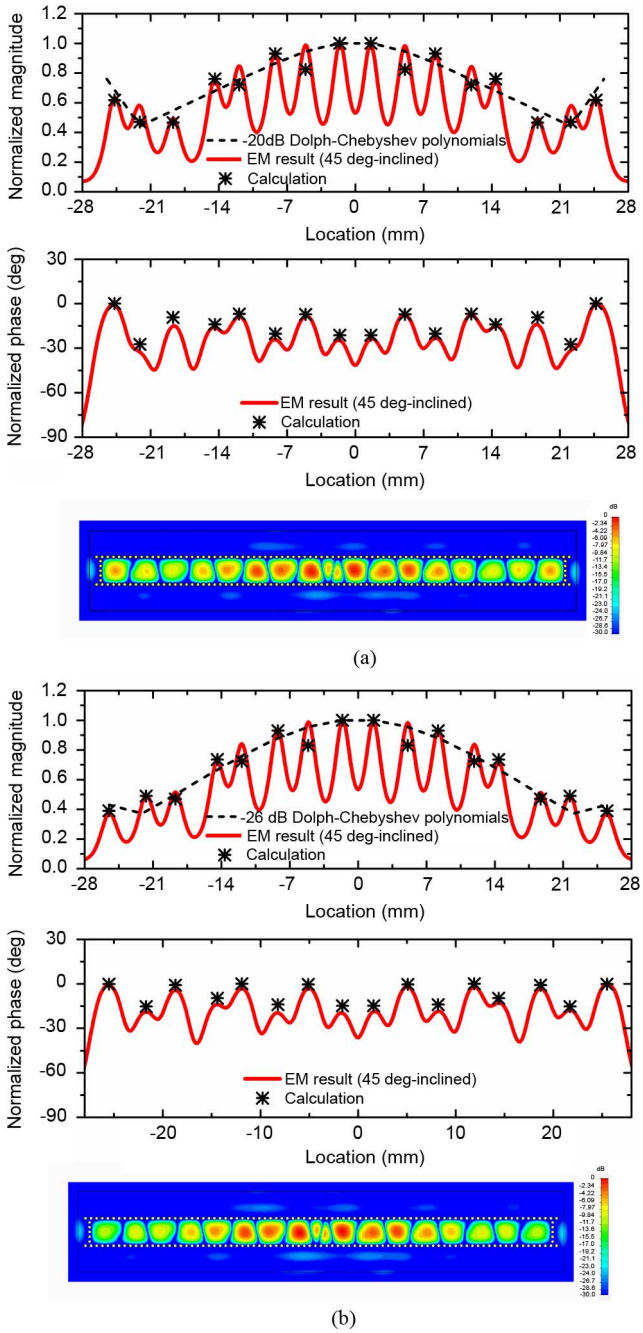

Fig. 5. Excitation coefficient design results for (a) –20 dB and (b) –26 dB, respectively, with electric field distribution (E_z) inside a radiating SIW.

TABLE I
THE DESIGN PARAMETERS AND OPTIMIZED VALUES

Axial displacements	x_1		x_2		x_3
Value	0.8*	0**	0*	0.4**	0
	x_4	x_5	x_6	x_7	x_8
	0.8	0	0.25	0	0.2
Radiating slot length	*Inductive slot* (l_i)		*Capacitive slot* (l_c)		*Slot width*
Value	2.24		3.58		0.4
Coupling slot	*Tilt angle*		*Slot length*		*Slot width*
Value	15°		2.33		0.7

(Units: mm)
(* for –20 dB and ** for –26 dB SLL)

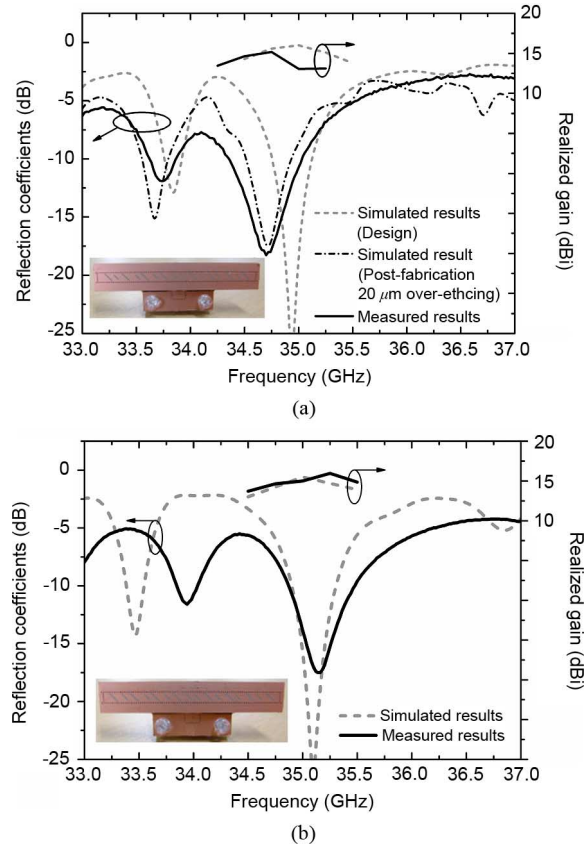

Fig. 6. The reflection coefficients and realized gain results with fabricated antenna pictures of (a) –20 dB SLL and (b) –26 dB SLL slot array antennas, respectively.

especially for the last two radiating slots, slots #1 and #16. Therefore, the capacitive slots #1 and #16 inevitably move in a positive direction (i.e., $x_1 = 0.8$ mm) without any movement of x_2, whereas the –26 dB SLL is relatively easy to design due to the gradually decreasing feature in this case. Hence, x_2 is set to 0.4 mm without any capacitive axial displacement. In addition, we calculate the slot voltages using an equivalent circuit model and compare the results to the EM simulation results, as shown in Fig. 5. The calculated voltage of capacitive slot #7 is slightly lower than the simulated result. Nevertheless, the error is hardly affects SLLs because of insignificant amount of error. The axial displacement amounts as well as the other design parameters, such as the length of the radiating slots and the series-to-series coupling slot, are listed in Table I with their optimized values.

V. MEASURED RESULTS

The proposed design method for low SLL slot array antennas is verified from measurements of the reflection coefficient, realized gain, SLL, and XPD. The proposed antennas are fed from a wideband coax-to-SIW transition to provide the input power without any external electromagnetic coupling noise [9]. The reflection coefficients are measured using the N5230A network analyzer of Agilent Technologies. These are shown in Fig. 6 with the simulation results. The measured impedance bandwidths of the two types of SLLs respectively ranged from 34.36 to 35.04 GHz (Fig. 6(a)) and from 34.88 to 35.48 GHz (Fig. 6(b)) with a VSWR of less than 2:1 for the two cases. The measured center frequency of –20 dB SLL slot array antenna is slightly changed from 34.93 GHz to 34.7 GHz with 0.66% frequency shift error and the reflection is somewhat increased from –27 dB to –18 dB. This discrepancy is mainly due to etching error and thus the

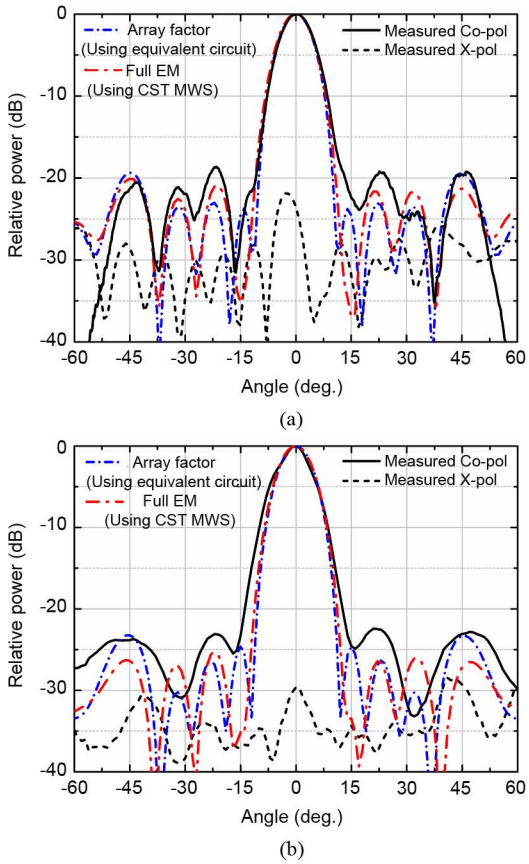

Fig. 7. The measured radiation patterns (zx plane) with calculated array factor and full-wave simulation results for 45°–inclined LP of two types of linear array antennas. (a) –20 dB SLL, (b) –26 dB SLL.

TABLE II
RADIATION CHARACTERISTICS FOR TWO TYPES OF ANTENNAS

Antenna type & Frequency		SLL (dB)	XPD (dB)	Gain (dBi)
-20 dB Antenna	*34.75 GHz*	–18.7	–26.92	15.17
	35.0 GHz	–16.6	–23.46	13.05
	35.25 GHz	–15.6	–23.99	13.11
-26 dB Antenna	*34.75 GHz*	–21.9	–28.39	14.64
	35.0 GHz	–22.5	–29.64	15
	35.25 GHz	–20.2	–23.41	15.95

post-fabrication simulation was conducted with 20 μm over-etched radiating and coupling slots for the proposed –20 dB SLL slot array antenna. As a result, the similar result with measured reflection coefficient was obtained for resonant frequency and reflection as shown in Fig. 6(a). Meanwhile, the measured resonant frequency of 35 GHz for –26 dB SLL slot array antenna in Fig. 6(b) shows similar tendency with simulation, even if there are some differences at lower frequency range.

The realized gain and radiation patterns are depicted in Figs. 6 and 7. The peak gains are 15.17 dBi at 34.75 GHz and 15.95 dBi at 35 GHz for the –20 dB and –26 dB SLL array antennas, respectively. Additionally, the proposed antennas show the high efficient radiation characteristics with the total efficiencies of 72.57% and 78.66%, respectively, at the center frequency of 35 GHz. Meanwhile, the calculated array factors using the calculated slot voltages presented in Fig. 5(a) and (b) are compared with the radiation patterns of CST MWS in Fig. 7. It is found that these calculated and the simulated results are well matched each other. Furthermore, even though there are phase variations about 27° and 15° among radiating elements for two types of antennas, respectively, the intended SLLs can be successfully realized. The measured SLLs are obtained with slightly increased levels of –18.7 dB and –22.5 dB, respectively, and the frequency variations of SLL are summarized in Table II including XPD and realized gain.

It is found that the x–directed electric currents on both long edges of a narrow upper metal plate are strongly induced from main radiating slots and ultimately increase cross-polarization levels. In addition, the diffracted and re-radiated fields from a protruded part of a lower PCB and a coaxial cable for measurement also increase the cross-polarization level, respectively. However, the optimum width of the upper metal plate can be obtained from full-wave EM simulation and is set for 80 mm ($= w$ in Fig. 1(b)) to suppress the cross-polarization. As a result, the lower cross-polarization levels of the proposed antennas are detected respectively as –26.92 dB and –29.64 dB at the boresight.

VI. CONCLUSIONS

An excitation control method for a series slot array antenna generating 45° linear polarization is proposed. With the use of axial displacement on each radiating slot along the center line of a broad wall of a SIW, the mode currents on each radiating slot can be controlled, which allows the arbitrary excitation coefficients to be determined. In addition, –20 dB and –26 dB linear slot array antennas are designed and fabricated for verification. It is expected that the proposed low sidelobe level design method for series slot array antennas can help one realize arbitrary radiation of 45°–inclined linear polarization.

REFERENCES

[1] H. Uchimura, T. Takenoshita, and M. Fujii, "Development of a "Laminated waveguide," *IEEE Trans. Microwave Theory Tech.*, vol. 46, no. 12, pp. 2438–2443, Dec. 1998.
[2] F. Xu and K. Wu, "Guided-wave and leakage characteristics of substrate integrated waveguide," *IEEE Trans. Microwave Theory Tech.*, vol. 53, no. 1, pp. 66–73, Jan. 2005.
[3] Y. J. Cheng, K. Wu, and W. Hong, "Power handling capability of substrate integrated waveguide interconnects and related transmission line systems," *IEEE Trans. Adv. Packag.*, vol. 31, no. 4, pp. 900–909, Nov. 2008.
[4] K. Hashimoto, J. Hirokawa, and M. Ando, "A post-wall waveguide center-feed parallel plate slot array antenna in the millimeter-wave band," *IEEE Trans. Antennas Propag.*, vol. 58, no. 11, pp. 3532–3538, Nov. 2010.
[5] J. Hirokawa and M. Ando, "45° linearly polarized post-wall waveguide-fed parallel-plate slot arrays," *Proc. Inst. Elect. Eng., Microw. Antennas Propag.*, vol. 147, no. 6, pp. 515–519, Dec. 2000.
[6] S. Park, Y. Okajima, J. Hirokawa, and M. Ando, "A slotted post-wall waveguide array with interdigital structure for 45° linear and dual polarization," *IEEE Trans. Antennas Propag.*, vol. 53, no. 9, pp. 2865–2871, Sep. 2005.
[7] X.-P Chen, K. Wu, L. Han, and F. He, "Low-cost high gain planar antenna array for 60-GHz band applications," *IEEE Trans. Antennas Propag.*, vol. 58, no. 6, pp. 2126–2129, Jun. 2010.
[8] D. Kim, W.-S. Chung, C.-H. Park, S.-J. Lee, and S. Nam, "Design of a 45°–inclined SIW resonant series slot array antenna for Ka band," *IEEE Antennas Wireless Propag. Lett.*, vol. 10, pp. 318–321, 2011.
[9] D. Kim, W.-S. Chung, C.-H. Park, S.-J. Lee, and S. Nam, "A series slot array antenna for 45°–inclined linear polarization with SIW technology," *IEEE Trans. Antennas Propag.*, vol. 60, no. 4, pp. 1785–1795, Apr. 2012.
[10] A. F. Stevenson, "Theory of slots in rectangular waveguides," *J. Appl. Phys.*, vol. 19, pp. 24–38, Jan. 1948.
[11] R. S. Elliott, "An improved design procedure for small arrays of shunt slots," *IEEE Trans. Antennas Propag.*, vol. AP–31, no. 1, pp. 48–53, Jan. 1983.
[12] M. Orefice and R. S. Elliott, "Design of waveguide-fed series slot arrays," *Proc. Inst. Elect. Eng.*, vol. 129, pp. 165–169, Aug. 1982.
[13] CST Microwave Studio (MWS) 2012, CST Corporation [Online]. Available: http://www.cst.com.